

Comparative Analysis of Ray Tracing and Rayleigh Fading Models for Distributed MIMO Systems in Industrial Environments

Aymen Jaziri*, David Demmer†, Yoann Corre*, Jean-Baptiste Doré†, Didier Le Ruyet‡,
Hmaied Shaiek‡, Pascal Chevalier‡

*SIRADEL, Saint-Grégoire France, ajaziri@siradel.com

† CEA-Leti, Université Grenoble Alpes, Grenoble, France, david.demmer@cea.fr

‡ CNAM, CEDRIC Laboratory, Paris, France, didier.le_ruyet@cnam.fr

Abstract—This paper presents a detailed analysis of coverage in a factory environment using realistic 3D map data to evaluate the benefits of Distributed MIMO (D-MIMO) over colocalized approach. Our study emphasizes the importance of network densification in enhancing D-MIMO performance, ensuring that User Equipment (UE) remains within range of multiple Access Points (APs). To assess MIMO capacity, we compare two propagation channel models: ray tracing and stochastic. While ray tracing provides accurate predictions by considering environmental details and consistent correlations within the MIMO response, stochastic models offer a more generalized and efficient approach. The analysis outlines the strengths and limitations of each model when applied to the simulation of the downlink (DL) and uplink (UL) single-user capacity in various D-MIMO deployment scenarios.

Index Terms—Ray tracing, Rayleigh fading, Smart factory, Distributed MIMO, Cell-Free massive MIMO, SVD, ZF.

I. INTRODUCTION

The introduction of private mobile networks is anticipated to revolutionize various industries, including factory automation, transportation and logistics sectors, significantly influencing their operations. Alongside advancements like Mobile Edge Computing (MEC), Time-Sensitive Networking (TSN), and improved security measures, Distributed Multiple Input Multiple Output (D-MIMO) technology is also expected to enhance communication availability and reliability in indoor settings, such as factories. This is achieved by increasing Line-of-Sight (LoS) coverage and lowering the chances of signal obstruction, as multiple Access Points (APs) can serve individual users.

In this paper, we characterize the MIMO propagation channel and present a detailed analysis of the impact of network densification on coverage overlapping and optical visibility. This is accomplished through the realistic modeling of 3D map data and Ray Tracing (RT) simulations in a factory setting, leveraging the 3.7 GHz spectrum, which is designed to deliver low-latency, high-capacity private 5G solutions [1]. Previous studies have underscored the importance of realistic propagation models in achieving reliable wireless communication in industrial settings [2], [3]. In this private network scenario, our objective is to evaluate the potential advantages that D-MIMO technology, in conjunction with network densification, can bring to indoor environments. D-MIMO systems rely on multiple APs to serve User Equipments (UEs) [4]. Enhanced coverage overlapping and improved optical visibility ensure that UEs are within the range of multiple APs, facilitating

the effective implementation of D-MIMO. Additionally, we aim to highlight the disparity between a fully RT-based channel model and the Rayleigh-based fading model that is commonly used in theoretical research. The theoretical benefits of D-MIMO and Cell-Free massive MIMO (CF-mMIMO) over conventional co-located MIMO and small non-cooperative base stations have been extensively investigated in the literature. For instance, a comparison between numerous non-cooperative small cells and CF-mMIMO is presented in [5]. These studies highlight the potential of D-MIMO and CF-mMIMO to provide superior coverage, increased capacity, and enhanced reliability, making them promising solutions for future wireless communication networks. Despite extensive research into D-MIMO communications, few studies have evaluated the combined impact of network densification and D-MIMO on network performance using realistic RT propagation data (e.g. [6] for mmWave). This work, therefore, contributes to the evaluation of propagation in an industrial environment based on RT tools and assesses system performance by incorporating a physical layer model capable of advanced, state-of-the-art processing, such as uplink (UL) cooperative detection and downlink (DL) cooperative beamforming for multi-stream transmissions.

This paper is structured as follows. Section II briefly explains the studied scenario and the considered propagation channel models. Section III details the system model, the power allocation and the spectral efficiency computation. Section IV presents the numerical results and analysis. Finally, Section V concludes the paper and gives future perspective of this work.

II. SYSTEM MODEL

We consider $M \times N$ distributed Multiple Input Multiple Output (MIMO) Orthogonal Frequency Division Multiplexing (OFDM) transmission with N_c sub-carriers. The APs and UEs operate under a Time Division Duplexing (TDD) protocol, which consists of an UL pilot training phase for channel estimation, an UL transmission and a DL transmission. We assume perfect synchronization among APs in terms of time, frequency, and phase. Additionally, channel reciprocity between UL and DL links is considered, enabling the MIMO system to operate in closed-loop mode with Channel State Information (CSI) available at the transmitter. The UL channel

estimation can thus be used to determine the DL precoding coefficients.

The received signal vector $\mathbf{y}_k \in \mathbb{C}^{N \times 1}$ at the k -th subcarrier can be written as

$$\mathbf{y}_k = \mathbf{W}_k \left(\mathbf{H}_k \sqrt{\mathbf{P}_k} \mathbf{F}_k \mathbf{Q}_k \mathbf{x}_k + \mathbf{n}_k \right), \quad (1)$$

where $\mathbf{x}_k \in \mathbb{C}^{N \times 1}$ is the transmitted signal, $\mathbf{n}_k \in \mathbb{C}^{N \times 1}$ the noise vector. Each element of the noise vector is uncorrelated and follows a normal distribution, specifically $\mathcal{N}(0, N_0)$. $\mathbf{W}_k \in \mathbb{C}^{N \times N}$, $\mathbf{H}_k \in \mathbb{C}^{M \times N}$, $\mathbf{P}_k \in \mathbb{R}^{M \times M}$, $\mathbf{F}_k \in \mathbb{C}^{M \times N}$ and $\mathbf{Q}_k \in \mathbb{C}^{N \times N}$ are respectively the linear combining at the receiver side, the propagation channel matrix, the per-antenna amplification gains (diagonal matrix), the linear precoding applied at the transmitter side and the per-layer power allocation (diagonal matrix)¹. In this work, we consider Single-User (SU) multi-layer transmissions meaning that independent data streams are transmitted in parallel. Therefore, the precoding/combining techniques aim at isolating the different independent streams and avoid inter-layer interference. Two strategies are considered for DL: i) the Zero forcing (ZF) where $\mathbf{F}_k \triangleq \mathbf{H}_k^\dagger$ ² and \mathbf{W}_k is the identity matrix and ii) the Singular Value decomposition (SVD) where $\mathbf{F}_k \triangleq \mathbf{U}_k^H$ and $\mathbf{W}_k \triangleq \mathbf{V}_k$ for $\mathbf{H}_k = \mathbf{V}_k^H \mathbf{\Sigma}_k \mathbf{U}_k$. The main difference between the two approaches is the presence of a combiner for SVD. We assume that combiners \mathbf{W}_k are either supplied to or estimated by the UEs. In this scenario, the number of UE received antennas matches the number of multiplexed MIMO layers. For both techniques, a water-filling algorithm is applied to each carrier. Power allocation is achieved in a way maximizing the achievable capacity [7].

The proposed study aims at comparing the achieved performance of legacy co-localized and distributed architectures. Indeed, in co-localized scenarios, when the UEs are served by a unique AP, M denotes the number of AP antennas. On the other hand, with distributed architectures, M denotes the total numbers of active antennas (*i.e.* number of cooperative APs times the number of antenna per AP). Indeed, we assume centralized processing, meaning that the DL precoding is computed from the CSI of all APs. This deployment strategy relies on a potential heavy fronthaul use because Distributed Unit (DU) and Radio Units (RUs) continuously exchange data streams and signaling. Local precoding [8], [9] provides better scalability but will not be addressed in the proposed paper and left as a perspective study. In this work, we consider a small-scale deployment (indoor factory) with a limited number of deployed APs (15 max) which is compatible with centralized processing. Additionally, perfect CSI is assumed for theoretical performance evaluation. For the UL, we assume no precoding at the UE transmitter side and employ a centralized ZF detector for signal detection.

III. CHANNEL MODELS

A. Propagation scenario

For our evaluation and comparison, we use a digital model of a factory area of size 97×36 m². As depicted in Fig. 1,

¹As channel aging is not considered in the proposed study, we decided to omit the time indices for sake of simplicity.

²where x^\dagger denotes the right Moore-Penrose pseudo inverse of x

the area is like a warehouse that is furnished with many metal racks of height 4 meters. In this scenario, we generate a massive MIMO channel samples database. The 15 considered APs are placed at 5 meters above the ground (just under the ceiling) and 1 meter away from walls. The 679 UEs are uniformly distributed in a grid with a resolution of 2 meters over the study area, resulting in a density of 0.25 UE/m². All users are positioned at height of 1.5 meters above the ground. Channel predictions are made for APs and UEs equipped with dual-polar (V/H) antenna arrays operating at 3.7 GHz.

B. Ray tracing model

The in-factory propagation is first simulated using the Volcano RT tool [3], which is capable of handling complex 3D indoor scenarios and efficiently scaling to a large number of UEs. The number of allowed interactions, *i.e.* two reflections and one diffraction along each ray-path, is a trade-off between computation time and accuracy of the predicted channels that was previously tested in a factory environment [10]. RT is used to generate both the average path-loss and the wideband MIMO matrix for each AP-UE link. As the considered antennas are dual-polarized, a particular attention is given to accurate modelling of the depolarization. A specific calibration work is conducted for adjustment of two correction parameters (a multiplicative factor and an offset) applied to the cross-polarization ratio (XPR) of each interaction. Two reliable sources are considered: the 3GPP InF model [11]; and dual-polar measurements recently collected in a machine room [12]. In the 3GPP model, a random XPR is applied independently to each ray, with an average of 12 dB in Line-of-Sight (LoS) and 11 dB in Non Line-of-Sight (NLoS). The standard deviation is 6 dB for both optical visibilities. As well, the dual-polar measurements indicate an XPR in the range of 10 – 12 dB [12]. The RT calibration is performed such that the corrected XPR's fall into the target range. Note that we also considered a cross-polar discrimination of 20 dB at the transmit and receive antennas, leading to possible additional depolarization.

As the system level simulations are realized for 20 MHz of bandwidth, we evaluate the channel coherence bandwidth in order to understand the frequency range over which the channel can be considered flat and determine the number of frequencies to be simulated in the synthetic MIMO channel matrices. The results from the predictions showed that the coherence bandwidth for 90% of the considered links with Single Input Single Output (SISO) path-loss smaller than 170 dB is higher than 371 kHz (almost equivalent to 1 resource block (RB) in the 5G NR when the numerology is equal to 1). So, in the channel samples database, a MIMO channel matrix is computed for each resource block.

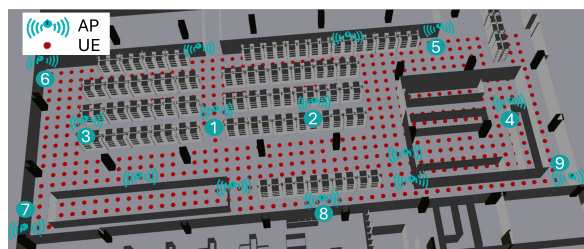


Fig. 1. Study area with the 15 APs and 679 possible UEs.

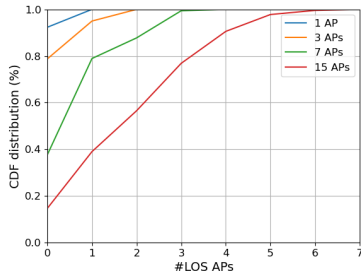


Fig. 2. CDF of the number of LoS APs per UE.

C. Stochastic-based fading model

To compare with the RT-based predictions, we also consider a Rayleigh stochastic model for generation of the MIMO channel coefficients. This model is built upon the RT path-loss characteristics. Indeed, on average the Rayleigh channels generated for a given link experiences the same channel gains and polarization diversity than in the RT prediction. Then, the variation of the channel coefficients along the bandwidth and antenna pairs are randomly selected from a complex normal distribution, scaled by the sub-carrier power model given by RT; $\mathbf{H}_k^{Rayleigh}(n, m) = |\mathbf{H}_k^{RT}(n, m)| \times \mathbf{s}_k(n, m)$, $\mathbf{s}_k(n, m) \in \mathcal{CN}(0, 1)$. It ensures perfectly independent frequency and spatial channel coefficients; the later characteristics is usually beneficial to the MIMO capacity.

IV. NUMERICAL SIMULATIONS

In this section, we use the two channel models to evaluate D-MIMO deployments. First, we present a statistical analysis of the radio propagation conditions met in the considered scenario, based on the RT site-specific prediction for four distinct network designs (indexed in the map Fig. 1):

- Single AP: Id 1
- 3 APs: Id 2,3,4
- 7 APs: Id 1,4,5,6,7,8,9
- 15 APs: All.

A. Propagation analysis

We present a variety of propagation coverage performance metrics and analyses, all of which result from the previously mentioned network designs. Our primary objective is to provide a comprehensive overview of the anticipated performance enhancements resulting from network densification, as well as the influence of other network parameters. In Fig. 2, we plot the Cumulative Distribution Function (CDF) of the number of LoS APs to a UEs of the study area. We observe that with only one AP (the blue curve), more than 90% of the UEs are in NLoS. This indicates that a single AP is insufficient to provide reliable LoS coverage to the majority of UEs. However, with the densification of the network, the percentage of LoS to one or more APs increases significantly. For instance, in the design with 7 APs, 40% UEs are still in NLoS from any activated APs, 40% UEs are in LoS with one AP and 20% UEs are in LoS with at least two APs. Furthermore, for the design with 15 APs, more than 40% UEs are in LoS with at least 3 APs. This CDF is a measure of the LoS diversity offered by multi-AP connectivity.

To further elucidate the benefits derived from network densification, and understand the impact of the transmit (Tx)

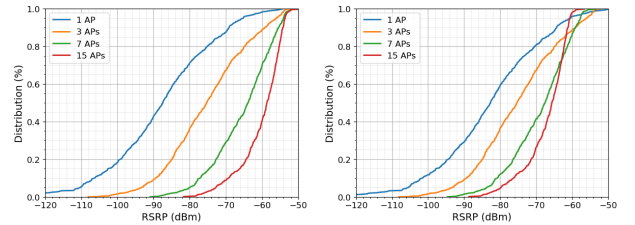


Fig. 3. CDF of the best-server RSRP, for constant AP Tx power (left), or constant network Tx power (right).

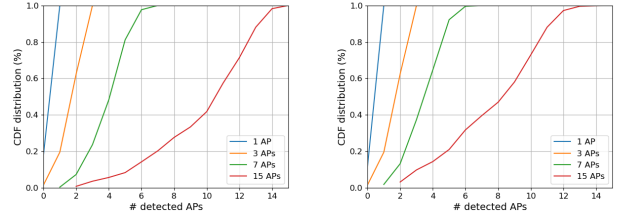


Fig. 4. CDF of the number of detected APs, for constant AP Tx power (left), or constant network Tx power (right).

power distribution among APs, we propose an examination of two distinct Tx power models: first, with a constant total Tx power per AP *i.e.* 23 dBm for 20 MHz bandwidth; second, with a constant Tx power for the entire network *i.e.* 27.8 dBm (equivalent to the sum of 3 APs in the previous approach). In Fig. 3, we plot the CDF of the Reference Signal Received Power (RSRP) from the best serving AP to each UE. As expected, when AP Tx power is constant, the network densification significantly enhances the best-server RSRP. However, the improvement gap narrows when considering more than 7 APs. At constant network Tx power, the densification leads to a smaller but still marked RSRP improvement, especially at lower levels. The impact on highest RSRP levels, typically above -65 dBm, may be negligible, even negative. Whatever the Tx power strategy, the densification promotes more uniform coverage performance, as indicated by the narrower RSRP distribution.

Fig. 4 shows the distribution of the number of detected APs per UE considering an RSRP threshold of -100 dBm. For both Tx power models, the densification allows to significantly improve the coverage (at least one AP detected). More than 80% UEs detect at least 2 different APs for both Tx power models when the network is composed of at least 7 APs. These results have significant impact on D-MIMO systems, which leverage multiple APs to serve UEs simultaneously, exploiting spatial diversity and reducing interference. The performance depends on APs overlap, thus on both the network density and power distribution strategy.

Fig. 5 illustrates the relative RSRP of the 2nd and 3rd best-serving APs compared to the highest RSRP. Close to 0 dB, the spatial diversity offered by the multi-AP connectivity is more likely able to provide several parallel streams of equivalent capacity. This evaluation helps to determine the suitability of deploying D-MIMO in a given scenario. As anticipated, the relative RSRP decreases significantly with densification. For instance, the relative RSRP of the 2nd best-server is above -10 dB for about 70% UEs when considering maximum densification, but for only 45% with 7 APs. The impact is

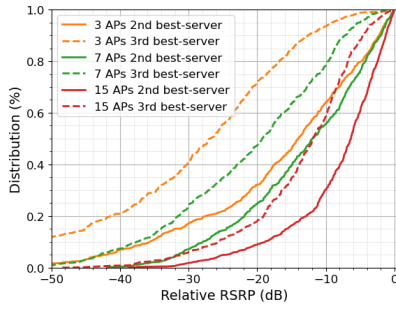


Fig. 5. Distribution of the relative RSRP for second and third best-serving APs.

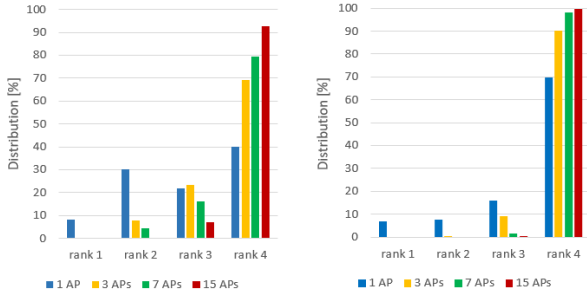


Fig. 6. MIMO channel rank distribution for RT prediction (left) and Rayleigh distribution (right).

even more pronounced for the third best AP.

The above results are valid for both the RT and stochastic channel models, since only the average power was considered. However, that changes when dealing with the distribution of the MIMO channel ranks, as presented by Fig. 6. The channel rank corresponds to the number of significant streams (*i.e.* with a received power greater than -100 dBm/RB) assuming a uniform power allocation of 17 dBm for the 4 antenna elements at the AP side. The channel rank is evaluated for the best-server only of each UE according to the different AP groups. First, one can observe that most of the channels admits a rank greater or equal to 2 thanks to the polarization diversity. Besides, densifying the network improves the channel matrix rank as it increases the stream powers by reducing the AP-UE distance. Regarding Rayleigh distribution, it provides the best proportion of full-rank matrices thanks to the absence of spatial correlation and therefore enhances link channel diversity (except for single-AP poor-quality links at rank 1).

Based on this characterized propagation environment, we are now studying the capacity of DL and UL transmissions.

B. UL Cooperative detection

We evaluate the performance of multi-layer SU-MIMO transmissions for the UL with 52 RBs. It's worth mentioning that RT provides a model at the RB scale. Consequently, simulations are conducted at the RB level, while performance measurements (capacity) are provided at the sub-carrier level (where 12 sub-carriers constitute one RB). The UE transmits 4-layers with a total power of 23 dBm, *i.e.* 17 dBm per antenna. Besides, 4-element Uniform Linear Arrays (ULAs) are considered for each AP and for UE. Among the 4 antennas, 2 are H-polarized, and the other 2 are V-polarized.

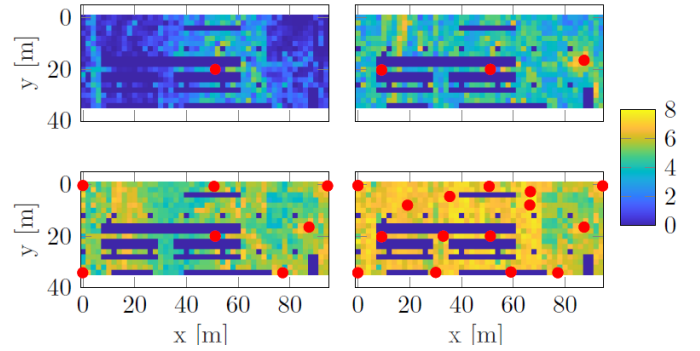


Fig. 7. Capacity [bits/s/Hz] map for UL 4-layer transmissions and the 4 deployment scenarios ($N_0 = -118$ dBm/RB).

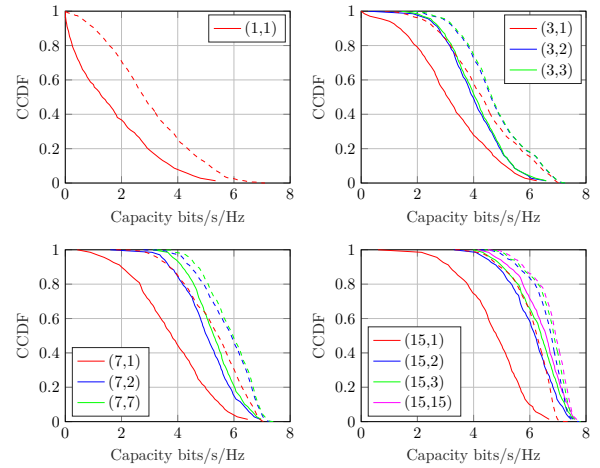


Fig. 8. CCDF of the capacity for 4-layers transmission. The dotted lines represent the Rayleigh channel model, while the solid lines correspond to the RT model ($N_0 = -118$ dBm/RB).

The co-polarized antennas are separated by $\lambda/2$ (where λ is the wavelength). The cross polarization between antennas is simulated with a cross polar discrimination equal to 20 dB. For illustration, Fig.7 presents the capacity map for quad-layer transmissions, RT channel model and four deployments (1, 3, 7 and 15 APs). Since graphical representations can be challenging to compare across different configurations, a statistical analysis is preferred.

Fig. 8 shows the Complementary Cumulative Distribution Function (CCDF) of the capacity per sub-carrier for both the RT and Rayleigh modes with different levels of cooperation. The configuration are labeled (a, b) : b APs are active among a possible. The selection of which APs to use is based on the strength of the received signal power. This criterion is advantageous due to its simplicity. However, other criteria, such as those based on the rank of the channel matrix, can be considered but would introduce additional computational complexity. In the single AP scenario, the Rayleigh model, being richer in diversity, demonstrates better performance. In the case of cooperation, we clearly observe the benefit of distributing antennas to exploit diversity. There is a threshold effect: beyond a certain number of cooperating APs, no further diversity gain is achieved. Since the selection of the number of cooperating APs is based on the received power metric,

increasing cooperation beyond 3 APs brings limited benefit. This is because we reach a certain level of diversity, and the focus is primarily on users close to the APs, resulting in channels that are predominantly LoS and have a good Signal-to-Noise Ratio (SNR). The Rayleigh model shows the same trends for this scenario and remains optimistic compared to RT.

C. DL Cooperative single user beamforming

We evaluate the performance of multi-layer DL SU-MIMO transmissions. It means that for each time/frequency resource only one UE is served by several independent datastreams (2 or 4 in this evaluation).

For the following numerical simulations, we consider a total transmit power fixed to 23 dBm to be spread over all available APs and antennas. As a consequence, varying the number of active APs changes the number of active antennas but keeps the same transmit power at the network level equal to 23 dBm. The AP antenna array is the same one considered for the UL study. The UEs are equipped with 2 and 4 antennas, thus are able to receive 2 (resp. 4) symbols streams (layers).

The evaluation of the median capacities is given in Fig.9. In two-layer transmissions, densifying the network increases the achievable capacity. Besides, AP cooperation is beneficial when a low number of serving APs is considered. Indeed, we observed with Fig.6 that most of the predicted channel matrix admit a rank of at least 2 which corresponds to the two polarizations. There is thus no need of spatial diversity which explains why joint transmission does not provide better results. This analysis is valid for both the ZF and SVD precoders and both the RT and Rayleigh channels. It seems worth noticing that the capacity does not decrease with the number of serving APs, and thus is not degraded due to the reduced power per antenna, thanks to the sum-power constraint considered at the network level.

When it comes to the quad-layer transmissions, one can also observe that densifying the network improves the network capacity. AP cooperation can also enhance the capacity especially for RT because there are less full-rank channel matrices with one serving AP as observed with Fig. 6. There is then a need of extra spatial diversity to properly multiplex the 4 datastreams. It is achieved with a limited number of serving APs. In terms of precoding techniques, SVD precoding offers better performance compared to ZF, mainly due to the effectiveness of the applied postcoder/combiner.

V. CONCLUSION

In this paper, we have presented a comprehensive analysis of coverage and capacity results in a single-user factory scenario using D-MIMO concept and realistic RT-based path-loss (including polarization diversity). The spatial fading component is derived either from RT or a stochastic Rayleigh model. The overall performance and behavior trends are quite similar across both channel models. However, the stochastic approach is found to be optimistic compared to RT, especially when no spatial correlation is considered which is frequently assumed in most D-MIMO numerical studies. Besides, network densification significantly enhances performance in both UL and DL. Although densification and cooperation are distinct

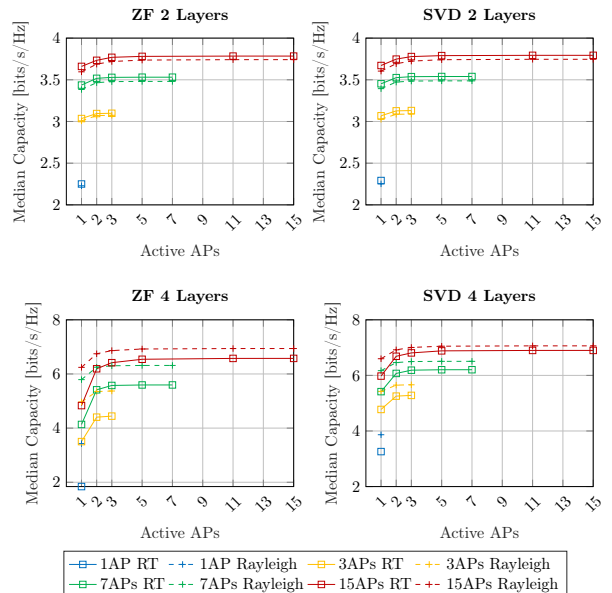


Fig. 9. Median capacity for different configuration and RT channel model with $N_0 = -118$ dBm/RB.

concepts, effective densification combined with limited cooperation, involving a small number of APs, is often sufficient to substantially optimize performance. It also emphasizes the crucial role of clustering strategies in improving overall network performance.

ACKNOWLEDGMENT

Part of this work received funding from the French National Research Agency within the frame of the project POSEIDON (ANR-22-CE25-0015).

REFERENCES

- [1] J.-B. Doré *et al.*, “ANR-POSEIDON Deliverable D1.1: Scenario description KPIs and PHY requirements, Tech. Rep. D1.1, Sept. 2023. [Online]. Available: <https://cea.hal.science/cea-04213326>
- [2] H. Ozawa, T. Fujimoto, and M. Katayama, “Modeling of sub-GHz wave propagation in factories for reliable wireless communication,” in *2018 IEEE International Conference on Industrial Technology (ICIT)*, 2018.
- [3] G. Gougeon, F. Munoz, Y. Corre, and R. D’Errico, “Ray-Tracing Calibration from Channel Sounding Measurements in a Millimeter-Wave Industrial Scenario,” in *2024 18th European Conference on Antennas and Propagation (EuCAP)*, 2024, pp. 1–5.
- [4] G. Hao, W. Henk, and M. Behrooz, “Integrated Communication, Localization, and Sensing in 6G D-MIMO Networks,” *arXiv preprint*, 2024.
- [5] H. Q. Ngo *et al.*, “Cell-Free Massive MIMO Versus Small Cells,” *IEEE Transactions on Wireless Communications*, vol. 16, no. 3, 2017.
- [6] H. T. da Silva *et al.*, “Evaluation of Cell-Free Millimeter-Wave Massive MIMO Systems Based on Site-Specific Ray Tracing Simulations,” vol. 10, pp. 82 092–82 105, 2022.
- [7] Proakis, *Digital Communications 5th Edition*. McGraw Hill, 2007.
- [8] E. Björnson and L. Sanguinetti, “Scalable Cell-Free Massive MIMO Systems,” *IEEE Transactions on Communications*, 2020.
- [9] G. Interdonato *et al.*, “Local Partial Zero-Forcing Precoding for Cell-Free Massive MIMO,” *IEEE Transactions on Wireless Communications*, 2020.
- [10] G. S. Bhatia, Y. Corre, and M. Di Renzo, “Efficient ray-tracing channel emulation in industrial environments: An analysis of propagation model impact,” in *in Proc. Joint European Conference on Networks and Communications (EuCNC/6G Summit)*, 2023, pp. 180–185.
- [11] 3GPP, “5G; Study on channel model for frequencies from 0.5 to 100 GHz,” 3rd Generation Partnership Project (3GPP), Technical Report (TR) 38.901, Jan 2020, version 16.1.0.
- [12] F. Munoz, G. Gougeon, Y. Corre, and R. D’Errico, “Millimeter-Wave Backscatter Channel Modelling for Sensing Applications in an Industrial Scenario,” *accepted in proceeding of EuCAP 2025*.